Electrochemical Synthesis of Mo_2C Catalytical Coatings for the Water-Gas Shift Reaction

Sergey A. Kuznetsov[a], Anton R. Dubrovskiy[a], Evgeny V. Rebrov[b], and Jaap C. Schouten[b]

[a] Institute of Chemistry, Kola Science Centre RAS, 14 Fersman Str., 184209 Apatity, Murmansk Region, Russia

[b] Laboratory of Chemical Reactor Engineering, Eindhoven University of Technology, P. O. Box 513, Eindhoven, The Netherlands

Reprint requests to S. A. K.; Fax: +7 815 55 61658; E-mail: kuznet@chemy.kolasc.net.ru

Z. Naturforsch. **62a,** 647 – 654 (2007); received May 23, 2007

Presented at the EUCHEM Conference on Molten Salts and Ionic Liquids, Hammamet, Tunisia, September 16 – 22, 2006.

The electroreduction of CO_3^{2-} ions on a molybdenum cathode in a NaCl-KCl-Li_2CO_3 melt was studied by cyclic voltammetry. The electrochemical synthesis of Mo_2C on molybdenum substrates has been performed at 1123 K for 7 h with a cathodic current density of 5 mA cm^{-2}. If molybdenum carbide is present as a thin (ca. 500 nm) film on a molybdenum substrate (Mo_2C/Mo), its catalytic activity in the water gas-shift reaction is enhanced by at least an order of magnitude compared to that of the bulk Mo_2C phase.

Key words: Cyclic Voltammetry; Electrode Processes; Electrochemical Synthesis; Water-Gas Shift Reaction; Catalytic Activity.

1. Introduction

For portable and transport applications, the most convenient and economical way of hydrogen production is on-board reforming of hydrocarbon fuels in a fuel processor (FP) combined with a fuel cell (FC) stack, forming an integrated power supply device. In the reforming of gasoline or natural gas, a hydrogen-rich gas is produced with a carbon monoxide content of 10 – 12 vol%. Because CO is a poison for a proton exchange membrane FC catalyst, the water-gas shift (WGS) reaction is used to reduce its content to below 1 vol%, increasing the H_2 yield. The water-gas shift is the reaction of CO with H_2O to form CO_2 and H_2. Since the reaction is exothermic, the equilibrium CO conversion is highest at low temperature. A two-stage process is often used [1], and in industrial reactors Fe-Cr catalysts are used for high-temperature shift and Cu-ZnO-Al_2O_3 catalysts for low-temperature shift. A presently used commercial Cu-ZnO-Al_2O_3 WGS catalyst occupies ca. 70% of the total catalyst volume of a 50 kW FP and does not meet volume requirements needed for automotive FC applications. The efficient use of (micro)structured catalytic reactors requires a shaping of the catalyst usually by deposition of thin catalytic coatings at the walls of the reactor channels. The large geometrical surface area of the channels in a microstructured reactor provides a large interface area between the reactants and the coating, which improves the catalytic performance. The aim of the present study is the development new generations of highly active and stable catalytic coatings for the WGS reaction by application of high-temperature electrochemical synthesis in molten salts. Bulk molybdenum carbides have exhibited promising catalytic activity for the WGS reaction, which is superior to that of the commercially used catalysts.

The coatings of molybdenum carbide on metal substrates can be obtained by vacuum-plasma deposition [2], by heating a molybdenum substrate in CO atmosphere at 1003 K followed by an annealing step at 1973 K [3], by reduction of $Mo(CO)_6$ with hydrogen on a metal wire at 573 – 1073 K [4], and by oxidation of ammonium paramolybdate to molybdenum trioxide followed by its reduction in an equimolar mixture of methane and hydrogen [5]. Electrochemical synthesis of molybdenum carbide thin films in molten salts containing alkali metal carbonates and molybdenum compounds has been studied in the temperature range from 1073 to 1273 K [6 – 10]. However, the electrodepo-

0932–0784 / 07 / 1000–0647 $ 06.00

sition mechanism of submicron Mo_2C coatings on a molybdenum substrate from chloride-carbonate melts remains unknown and is a major focus of the present paper. We also compare the catalytic activity of the resulting Mo_2C/Mo coatings with that of the bulk Mo_2C phase [5] and a commercial Cu-ZnO-Al_2O_3 WGS catalyst.

2. Experimental

2.1. Synthesis of Mo_2C

Molybdenum sheets (99.99+ wt% Mo) of 40 mm length and 8 mm width, with a thickness of 100 μm were used in this study. Molybdenum samples were cleaned in xylene for 1 h to remove organic contaminations from the surface, and dried in an oven at 413 K. Carburization of molybdenum substrates was carried out in a melt containing 5 wt% Li_2CO_3 in an equimolar NaCl-KCl mixture. Sodium and potassium chlorides (Prolabo, 99.5 wt%) were dehydrated by continuous and progressive heating just above the melting point in a gaseous HCl atmosphere in quartz ampoules. The excess of HCl was removed from the melt by an argon flow. The salts were handled inside a high purity argon atmosphere in a glove box (water content < 2 ppm) and stored in sealed glass ampoules. Li_2CO_3 (chemically pure) was dried for 24 h at 473 K. Sodium and potassium chlorides were mixed in the required ratio, placed in a glassy carbon ampoule (SU-2000 type) and transferred to a sealed stainless steel retort. The latter was evacuated to a residual pressure of 0.67 Pa, first at room temperature and then stepwise at 473, 673, and 873 K. The cell was heated using a programmable furnace, and the temperature was measured using a Pt-Pt10Rh thermocouple. The retort was then filled with high purity argon (U-grade: < 3 ppm H_2O and < 2 ppm O_2) and the electrolyte was melted. Li_2CO_3 (5 wt%) was added to the NaCl-KCl equimolar melt. The molybdenum substrates were immersed in the melt through a special opening in the top part of the retort under inert atmosphere. Synthesis of Mo_2C on the molybdenum substrates was performed at 1123 K for 7 h with a cathodic current density of 5 mA cm^{-2}. The glassy carbon crucible served as anode. In the experiments, the samples were washed in distilled water and alcohol and weighed.

2.2. Electrochemical Cell

A VoltaLab-40 potentiostat, controlled by the VoltaMaster-4 software (version 6), was used in linear sweep voltammetry (LSV) and cyclic voltammetry (CV) experiments. The potential scan rate (v) was varied between $5 \cdot 10^{-3}$ and 2.0 V s^{-1}. The experiments were carried out in the temperature range 973 – 1123 K. The CV curves were recorded between -1.3 and 0.2 V at molybdenum and glassy carbon (GC) electrodes with a diameter of (1.5 ± 0.5) mm with respect to a platinum wire acting as a quasi-reference electrode (QRE), Pt-PtO_x-O^{2-} [11], and an Ag/NaCl-KCl-AgCl (2 wt%) reference electrode. The GC ampoule served as the counter electrode.

2.3. Catalyst Testing

Prior to the testing, the coatings were pretreated in a hydrogen flow for 2 h at 773 K with a temperature ramp of 5 K min^{-1}. Ten Mo_2C/Mo substrate plates were loaded in a microstructured reactor parallel to each other at a distance of 185 μm between the adjacent plates. The reactor was heated by a Carbolite electrical oven. Feed and effluent compositions were analyzed by an on-line Varian 3800 gas chromatograph equipped with a molecular sieve and Porapak Q columns and thermal conductivity detectors. The CO conversion was measured at atmospheric pressure and a temperature between 473 and 653 K. The kinetic data were obtained in the differential reactor mode at CO conversions below 15%.

3. Results and Discussion

3.1. Electrode Processes Accompanying the Electrodeposition of Molybdenum Carbides

Cathodic Processes

Voltammograms obtained in a NaCl-KCl-Li_2CO_3 melt at the molybdenum electrode at different polarization rates are shown in Figure 1. Three cathodic waves (R_1, R_2, and R_3) were detected on these voltammograms, and four peaks of electro-oxidation (Ox_1, Ox_2', Ox_2'', and Ox_3). The height of the wave R_1 slowly decreased with increasing scan rate and mostly disappeared at a polarization rate of 1.0 V s^{-1} (Fig. 1d). Wave R_1 at v above 0.1 V s^{-1} was very weak compared to wave R_2, which was observed at more negative potentials (Figs. 1a – d). Potentiostatic electrolysis at potentials corresponding to wave R_1 led to the formation of hexagonal Mo_2C (XRD data) at the molybdenum electrode.

The current density of the reduction process in the potential range of R_1 was very small due to the low

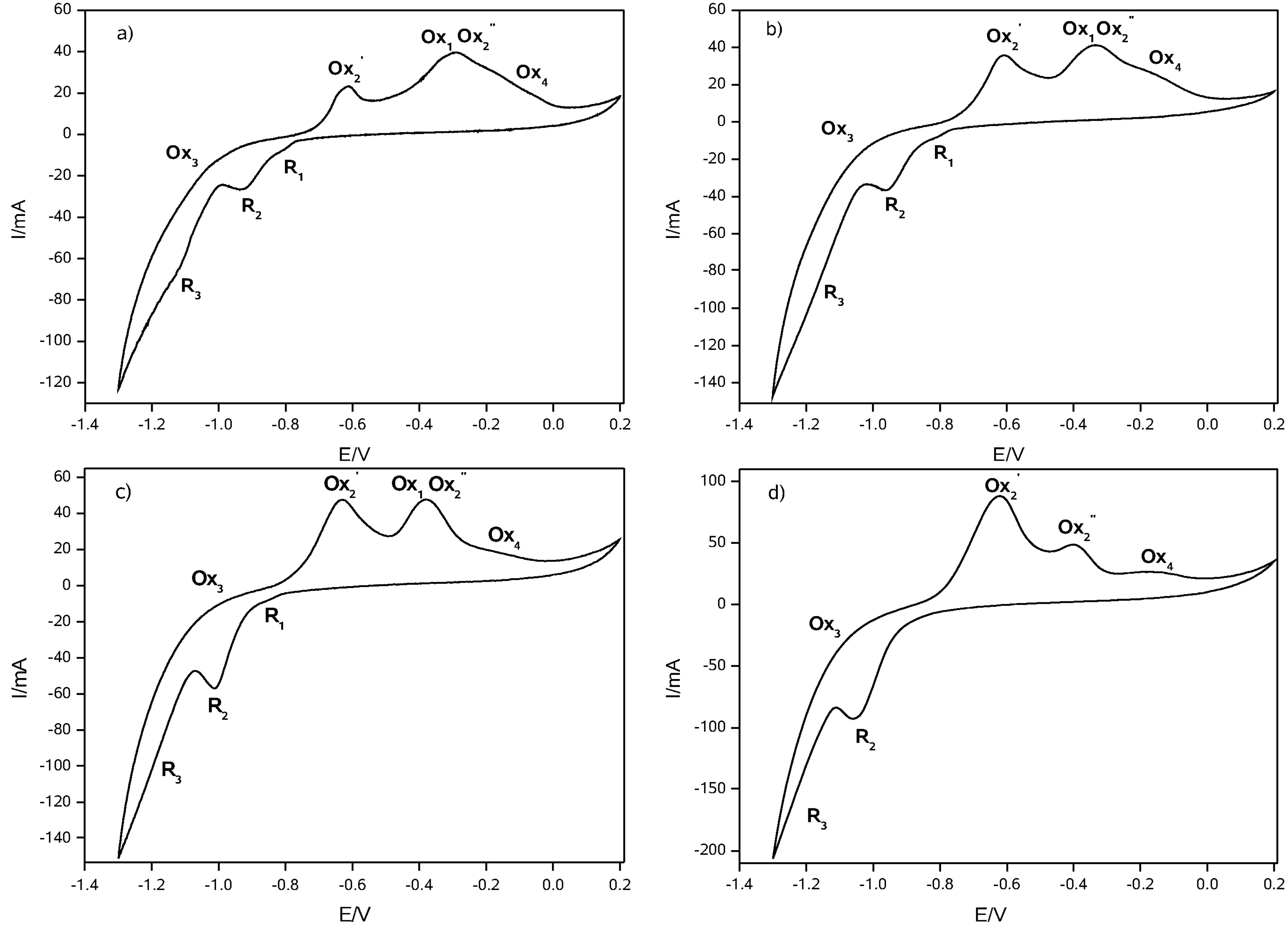

Fig. 1. Cyclic voltammograms at a molybdenum electrode in a NaCl-KCl-Li_2CO_3 melt. Electrode area: 0.238 cm^2. Sweep rates: (a) 0.1 V s^{-1}; (b) 0.2 V s^{-1}; (c) 0.3 V s^{-1}; (d) 1.0 V s^{-1}. Temperature: 1023 K. Concentration of Li_2CO_3: $2.37 \cdot 10^{-4}$ mol cm^{-3}. Quasi-reference electrode: platinum.

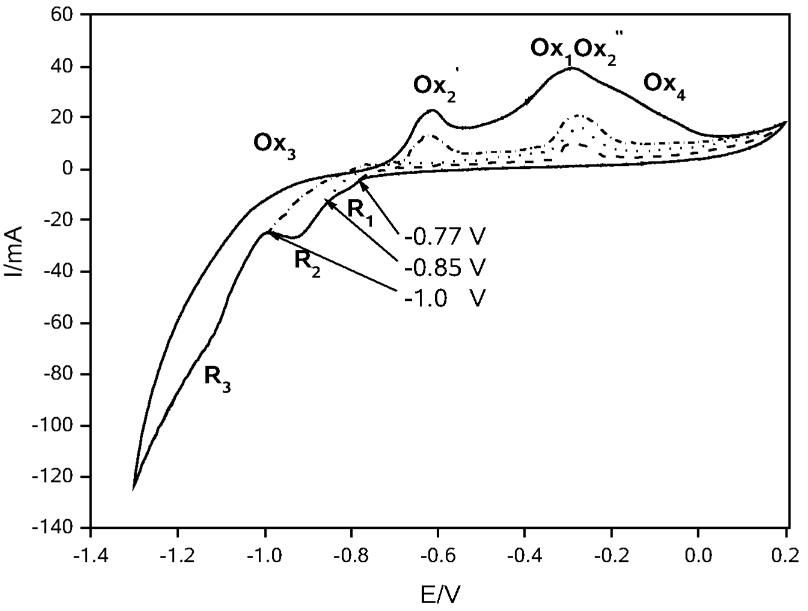

Fig. 2. Cyclic voltammogram at a molybdenum electrode in a NaCl-KCl-Li_2CO_3 melt at different reverse potentials. Electrode area: 0.238 cm^2. Sweep rate: 0.1 V s^{-1}. Temperature: 1023 K. Concentration of Li_2CO_3: $2.37 \cdot 10^{-4}$ mol cm^{-3}. Quasi-reference electrode: platinum.

concentration of carbon-containing species. This wave (R_1) is assigned to the reduction of carbon dioxide. Moreover the CO_2 solubility in an NaCl-KCl melt was around $(6-8) \cdot 10^{-8}$ mol cm^{-3} [12] and the electrode process can be described by the following reaction:

$$CO_2 + 4e^- + 2\,Mo \rightarrow Mo_2C + 2\,O^{2-}. \quad (1)$$

In the presence of carbonate species, reaction (1) is preceded by the chemical reaction

$$CO_3{}^{2-} \leftrightarrow CO_2 + O^{2-}. \quad (2)$$

Actually, the increase of the scan rate resulted in a decrease of the CO_2 concentration in the melt and the intensity of wave R_1 (Fig. 1). Therefore the electrode reaction (1) probably disappears at high polarization rates. Thus, process (1) is controlled by the preceding chemical reaction (2).

Mo_2C was found to be the only phase present in the coatings after potentiostatic electrolysis at the potential -0.850 V relative to the platinum quasi-reference electrode (Pt QRE) corresponding just to the start of wave R_2. In contrast, the MoC phase was formed with a negative shift of the electrolysis potential from -0.887 V towards the range of values corresponding to wave R_2. The electrode processes corresponding to wave R_2 are expressed by the following reactions:

$$CO_3{}^{2-} + 4e^- + 2\,Mo \rightarrow Mo_2C + 3\,O^{2-}, \quad (3)$$

$$CO_3{}^{2-} + 4e^- + Mo \rightarrow MoC + 3\,O^{2-}. \quad (4)$$

On the voltammetric curves it is not possible to distinguish between the processes (3) and (4), probably due to the close values of the discharge potentials for both reactions. The equilibrium potentials (E_{eq}) of the electrode processes were calculated from the standard Gibbs energy for the decomposition reaction:

$$E_{eq} = -\Delta G^0{}_T / nF, \quad (5)$$

where $\Delta G^0{}_T$ is the standard Gibbs energy at the temperature T for Li_2CO_3 decomposition into components with the formation of either Mo_2C or MoC, and n is the number of electrons involved in the corresponding electrode reactions. Thermodynamic data were taken for pure substances. Thermodynamic calculations confirmed the close values of the discharge potentials for the formation of the Mo_2C and MoC phases. Thus, the equilibrium potentials for the electrode reactions (3) and (4) at 1023 K were found to be -0.823 and -0.840 V, respectively, referred to the Ag/NaCl-KCl-AgCl (2 wt%) reference electrode.

At the same time, the peaks of both Mo_2C and MoC dissolution were clearly detected at the anodic half-cycle of the voltammograms (Figs. 1 and 2). Utilization of the reverse potentials corresponding to wave R_1 was accompanied by the oxidation wave Ox_1 only (Fig. 2). A reverse from the foot of wave R_2 (-0.850 V vs. Pt QRE) did not lead to a new oxidation wave, but

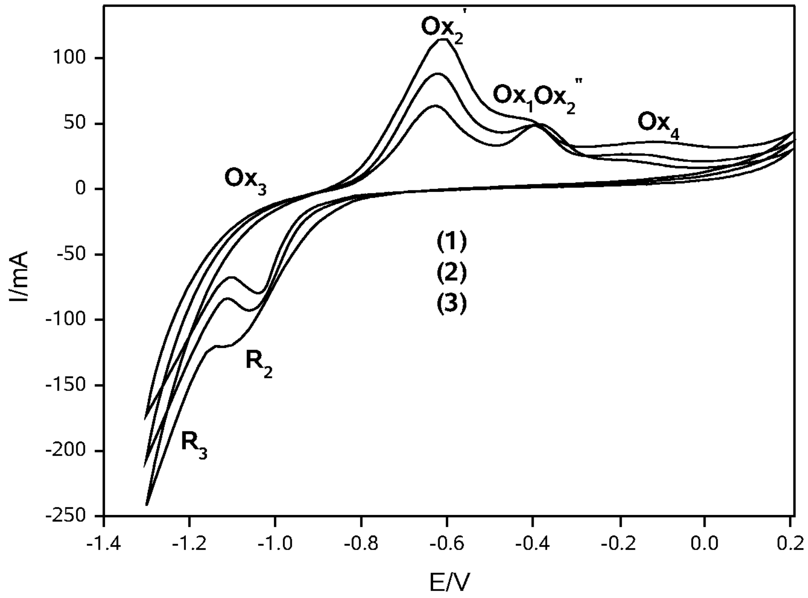

Fig. 3. Cyclic voltammograms at a molybdenum electrode in a NaCl-KCl-Li_2CO_3 melt. Electrode area: 0.238 cm^2. Sweep rates: (1) 0.5 V s^{-1}; (2) 1.0 V s^{-1}; (3) 2.0 V s^{-1}. Temperature: 1023 K. Concentration of Li_2CO_3: $2.37 \cdot 10^{-4}$ mol cm^{-3}. Quasi-reference electrode: platinum.

the height of the peak Ox_1 increased, implying that the Mo_2C phase was only formed on the molybdenum electrode in the cathodic half-cycle at these conditions, and waves Ox_2'' and Ox_1 had the same potential which corresponds to the dissolution of Mo_2C (Fig. 2). A new anodic peak (Ox_2') was observed in the anodic region when a more negative potential (−0.887 V vs. Pt QRE) was applied corresponding to the R_2 wave. This peak can be assigned to the dissolution of the MoC phase.

The peak current (R_2) of the CO_3^{2-} ions electroreduction was found to be directly proportional to $v^{1/2}$ in the scan rate range from 1.0 to 2.0 V s^{-1}, while the peak potentials shifted in the cathodic direction with increasing scan rate (Fig. 3). The electrode process of CO_3^{2-} reduction in the range of scan rates of 1.0 to 2.0 V s^{-1} is irreversible and controlled by the charge transfer as confirmed by the diagnostic criteria of linear sweep voltammetry [13]. Estimation of the value αn_α, where α is the charge transfer coefficient and n_α is the number of electrons transferred, is possible by applying the equation [14]

$$E_p{}^c - E_{p/2}{}^c = -1.857\mathrm{RT}/\alpha n_\alpha F, \qquad (6)$$

where $E_p{}^c$ is the potential of the cathodic peak and $E_{p/2}{}^c$ is the potential of the half peak. At a polarization rate of 1.0 V s^{-1}, the parameter αn_α was found to be 2.13.

The double layer charging current was virtually insignificant relative to the Faradayic current at a polarization rate of 1.0 V s^{-1} at 1023 K. Therefore, the diffusion coefficient of the CO_3^{2-} ions was determined utilizing the Delahay equation for an irreversible electrochemical process [15]:

$$I_p{}^c = 0.496nFCAD^{1/2}(\alpha n_\alpha F v/RT)^{1/2}, \qquad (7)$$

where $I_p{}^c$ is the peak cathodic current (A), A the electrode area (cm^2), C the bulk concentration of active species (mol cm^{-3}), D the diffusion coefficient (cm^2 s^{-1}), v the potential sweep rate (V s^{-1}), F the Faraday constant (C mol^{-1}), and T the absolute temperature (K).

The diffusion coefficient of carbonate ions at 1023 K was found to be $2.0 \cdot 10^{-6}$ cm^2 s^{-1}. This value is smaller than that reported in other studies [16–17]. It is likely that reactions (3) and (4), which are responsible for the electroreduction of the carbonate ions, are influenced by process (1) with preceding chemical reaction (2) even at relatively high polarization rates (1.0–2.0 V s^{-1}).

Waves R_3 and Ox_3 (Figs. 1–3) correspond to the discharge of alkali metal cations at the molybdenum cathode and the dissolution of alkali metals, respectively. The shoulder (Ox_4) on the voltammograms (Figs. 1–3) arises from the oxidation of oxide ions at the molybdenum surface, as it was confirmed by addition of Li_2O to the melt.

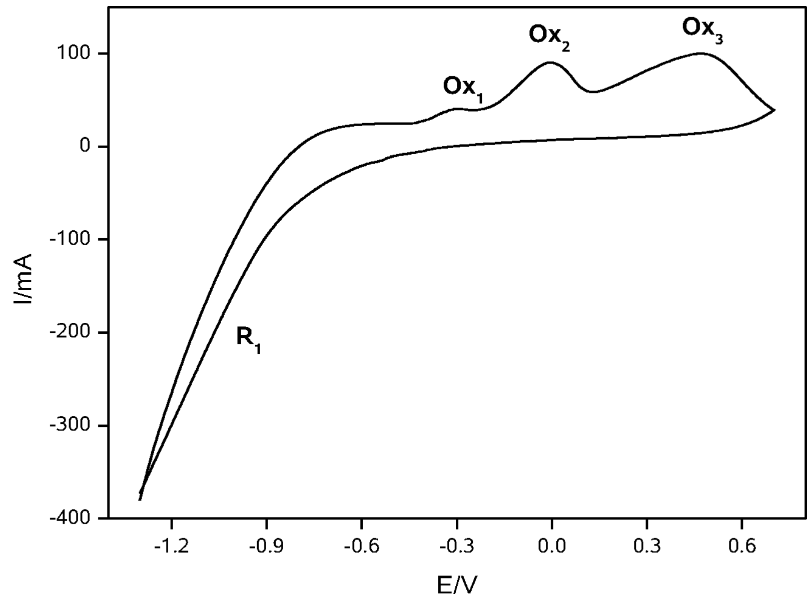

Fig. 4. Cyclic voltammogram at a glassy carbon electrode in a NaCl-KCl-Li_2CO_3 melt. Electrode area: 0.606 cm^2. Sweep rate: 0.5 V s^{-1}. Temperature: 1023 K. Concentration of Li_2CO_3: $2.37 \cdot 10^{-4}$ mol cm^{-3}. Quasi-reference electrode: platinum.

Anodic Processes

A cyclic voltammogram at the glassy carbon electrode is shown in Figure 4. A single ascending section was observed in the cathodic cycle of the voltammogram, while three oxidation waves were registered in the anodic part. After addition of oxide ions (Li_2O), the heights of the waves Ox_1 and Ox_2 increased while that of wave Ox_3 remained unchanged. However, the heights of all three oxidation waves increased with increasing Li_2CO_3 concentration. Based on this observation, one may conclude that the waves Ox_1 and Ox_2 are related to the oxidation of oxide ions, while wave Ox_3 can be assigned to the oxidation of carbonate ions. Similar variations of the height of the waves after addition of Li_2O and Li_2CO_3 were observed in [18, 19]. The anodic reaction of the oxide ions on a glassy carbon electrode can be described by a two-step scheme [18, 19]: electrochemical adsorption

$$O^{2-} + x\,C - 2e^- \rightarrow C_xO_{(ads)}, \qquad (8)$$

followed by electrochemical desorption

$$O^{2-} + C_xO_{(ads)} - 2e^- \rightarrow CO_{2(g)} + (x-1)\,C, \quad (9)$$

$$C_xO_{(ads)} \rightarrow n\,CO_{(g)} + m\,CO_{2(g)}, \qquad (10)$$

where $x = n + m$. The electrochemical process (9) is accompanied by thermal decomposition of the $C_xO_{(ads)}$ species via reaction (10). When the chlorine evolution potential is reached (+0.768 V vs. Pt QRE), $CO_{(g)}$ reacts with chlorine yielding phosgene ($COCl_2$) [19]. The oxidation of carbonate ions

$$2\,CO_3{}^{2-} + C - 4e^- \rightarrow 3\,CO_{2(g)} \qquad (11)$$

takes place at more positive potentials [19].

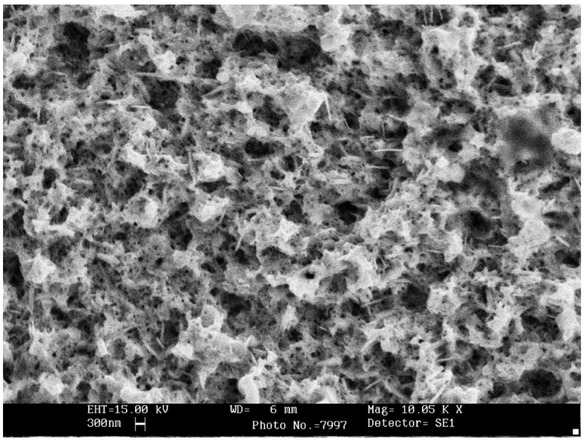

Fig. 5. Morphology of molybdenum carbide coating on a molybdenum substrate. Temperature: 1123 K. Current density: 5 mA cm^{-2}. Time of electrolysis: 7 h. Thickness: 0.5 μm.

During the electrochemical synthesis of Mo_2C, the anodic current density was below 1 mA cm^{-2}, therefore reactions (8) and (9) were the main anodic processes.

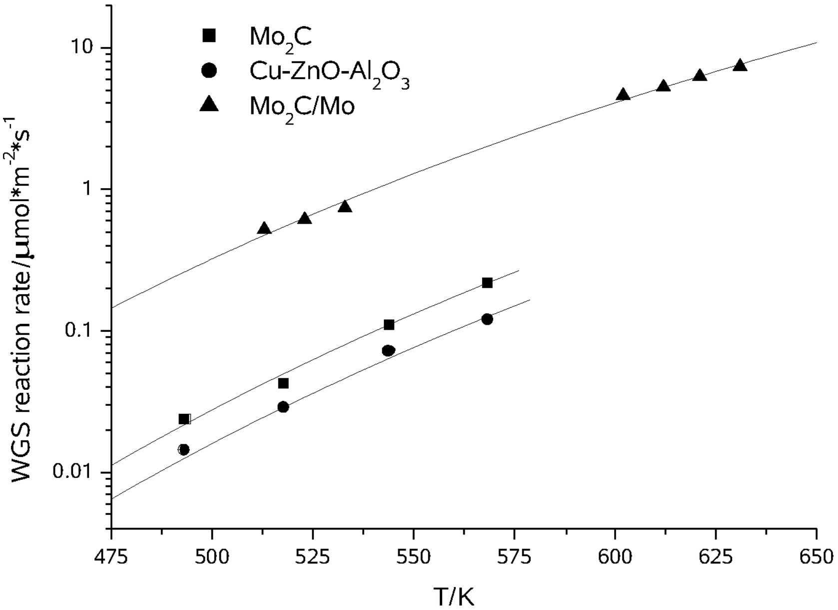

Fig. 6. Water-gas shift reaction rate as a function of temperature on different catalysts. p_{CO}, 0.003 atm; p_{H_2O}, 0.013 atm; p_{H_2}, 0.4 atm. Balance: He. Total flow: 50 cm^3 min^{-1} (STP).

3.2. Catalytic Activity of Mo_2C/Mo

The morphology of Mo_2C obtained at 1123 K from a $NaCl$-KCl-Li_2CO_3 (5 wt%) melt, for 7 h at a cathodic current density of 5 mA cm^{-2}, is presented in Figure 5. The specific surface area was determined by the BET method and was found to be 20 m^2 g^{-1}. The steady-state reaction rates for the Mo_2C/Mo coatings were higher than those for the bulk Mo_2C [5] and commercial Cu-ZnO-Al_2O_3 catalysts in the temperature range explored (Fig. 6). The catalytic activity was enhanced by at least an order of magnitude compared to that of the pure Mo_2C phase, if molybdenum carbides were present as a thin submicron layer on a molybdenum substrate. The methanation reaction was completely suppressed in the whole temperature range studied on the Mo_2C/Mo coatings. The catalytic activity remained constant during 500 h on-stream. The coatings were also stable during the thermal cycling, while the activity of commercial catalysts tends to decrease with time.

A detailed kinetic study is being carried out on the Mo_2C/Mo coatings. Based on the result of the kinetic study, an integrated microstructured reactor/heat-exchanger will be designed to further enhance the reaction yields by allowing the reactant stream to follow optimal reactant temperature profiles. The high-temperature electrochemical synthesis methods will be further developed towards the synthesis of molybdenum carbides on microstructured molybdenum substrates. The application of microstructured substrates with semi-cylindrical microchannels with a diameter of 150 – 200 microns will considerably enhance the geometrical area available for coating deposition compared to that of flat plates.

Acknowledgements

The financial support by the Netherlands Organization for Scientific Research (NWO), project No. 047.017.029, and by the Russian Foundation for Basic Research (RFBR), project No. 047.011.2005.016, is gratefully acknowledged.

[1] K. Kochloefl, Handbook of Heterogeneous Catalysis, VCH, Weinheim 1997.
[2] A. A. Andreev, L. V. Butalova, G. N. Kartmazov, T. V. Kostritsa, V. M. Lunev, and A. A. Romanov, Fiz. Khim. Obrab. Mater. **2**, 169 (1979).
[3] E. Gillet, J. C. Chiarena, and M. Gilet, Surf. Sci. **55**, 126 (1976).
[4] I. E. Campbell, C. F. Powell, D. H. Nowiski, and B. W. Gosner, J. Electrochem. Soc. **96**, 318 (1949).
[5] J. Patt, D. J. Moon, C. Phillips, and L. Tompson, Catal. Lett. **65**, 193 (2000).
[6] G. Weiss, Ann. Chim. **1**, 446 (1946).
[7] A. K. Suri, A. K. Mukherjee, and C. K. Gupta, J. Electrochem. Soc. **120**, 622 (1973).

[8] I. V. Shapoval, Kh. B. Kushkov, V. V. Malyshev, P. V. Nazarenko, and N. P. Baidan, Zashch. Met. **22**, 564 (1986).

[9] I. V. Shapoval, Kh. B. Kushkov, V. V. Malyshev, V. T. Vesna, and V. P. Maslov, Poroshk. Metall. **7**, 43 (1980).

[10] D. C. Topor and J. R. Selman, J. Electrochem. Soc. **135**, 384 (1988).

[11] C. Mamantov, Molten Salts: Characterizations and Analysis, M. Dekker, New York 1969.

[12] L. E. Ivanovskiy and V. N. Nekrasov, Gases and Ionic Melts, Nauka, Moscow 1979.

[13] R. S. Nicholson and I. Shain, Anal. Chem. **36**, 706 (1964).

[14] H. Matsuda and Y. Ayabe, Z. Elektrochem. **59**, 494 (1953).

[15] P. Delahay, New Instrumental Methods in Electrochemistry: Theory, Instrumentation and Application to Analytical and Physical Chemistry, Interscience, New York 1954.

[16] G. J. Janz and N. P. Bansal, J. Phys. Chem. Data **11**, 505 (1982).

[17] L. Massot, P. Chamelot, F. Bouyer, and P. Taxil, Electrochim. Acta **47**, 1949 (2000).

[18] V. I. Nekrasov, N. M. Barbin, and L. E. Ivanovskiy, Rasplavu **3**, 51 (1989).

[19] N. M. Barbin, Thesis, Institute of High Temperature Electrochemistry, Sverdlovsk, Russia 1987.